Theoretical and Experimental Investigation of Plane Wave Diffraction from an Amplitude Modified Fresnel Zone Plate

Ali Mohammad Khazaei[a], Fatemeh Afsharipour[b], Hamid Reza Mashayekhi[b], and Mohammad Yeganeh[c,*]

[a]Department of Physics, Lorestan University, Khorramabad, Iran
[b]Department of Interdisciplinary Physics and Technology, Faculty of Advanced Science and Technology, Shahid Bahonar University of Kerman, Kerman, Iran
[c]Department of Physics Education, Farhangian University, Tehran, Iran

Corresponding author email: m.yeghaneh@cfu.ac.ir

Regular Paper-Received: July 14, 2024 Revised: Sept. 08, 2024, Accepted: Sept. 10, 2024, Available Online: Sept. 12, 2024, DOI: 10.61186/ijop.17.2.195

ABSTRACT— A new class of gratings is produced by combining the radial grating (RG) with the Fresnel zone plate (FZP). Besides having an azimuthal periodicity, these gratings focus the incident beam at a specific distance. This paper investigated the diffraction from modified Fresnel zone gratings (MFZGs) theoretically and experimentally. Our approach was to solve the Fresnel-Kirchhoff integral in the cylindrical coordinate system for a plane beam on an MFZG. The experimental results of diffraction patterns of a laser beam from the amplitude type of MFZGs confirmed the theoretical predictions well. The near-field diffraction patterns agreed with the patterns obtained from theoretical calculations.

KEYWORDS: autofocusing, diffraction grating, Fresnel diffraction, Fresnel-Kirchhoff integral, radial grating.

I. INTRODUCTION

The wave is a fundamental aspect of nature, and light showcases one of its most exquisite effects. The diffraction phenomenon, evidence of light's wave nature, holds significance in physics and engineering fields related to wave propagation [1]. Creating one-dimensional light patterns is most easily achieved through the interference of two coherent beams. Another way to achieve different diffraction patterns is to use gratings which are common tools for this purpose [2]. Due to their periodic structure, diffraction gratings are optical components that induce light diffraction and result in light deviation at various angles. Linear gratings are the most known gratings, characterized by a one-dimensional periodic structure that can alter the amplitude or phase of the incident wave during transmission or reflection [3]. Gratings have various applications in optical science and related technologies. They are used in interferometry, spectrometry, moiré deflectometry, displacement measurement, etc. Gratings can be utilized in spectrometers, monochromators, and astronomical instruments like spectrographs to analyze the light emitted from celestial bodies for information on their composition, temperature, motion, and other properties [4]–[7]. RGs are another type of grating, where a set of lines extended radially from a common point is constructed, and the azimuthal angles corresponding to the adjacent lines are equal. The spatial periodicity increases with the radius in the azimuthal direction [8].

The FZP, designed by Fresnel in 1822, functions as a converging lens that focuses the incident beam at a specific distance. The diffraction grating based on the FZP also exhibits autofocusing properties [9]. FZP has been used in X-ray microscopy, spectroscopy, lithography, X-ray, and UV focusing when

acting as a lens and diffractive optical element with opaque and transparent rings. These applications are unattainable with refractive lenses due to their absorption [10].

In the last few decades, laser beam shaping has received much attention. Various beams, such as super Gaussian near top hat irradiance profile, the Airy beam, Laguerre-Gaussian beam, Mathieu beam, carpet beam, etc., can be produced by applying specific phases to the incident Gaussian beam. A specific phase is applied to the input beam using DOEs (diffracted optical elements), SLM (spatial light modulator), and phase plates. Such elements produce the mentioned beams through phase modulation [11]. Amplitude diffraction gratings can also create such beams through diffraction. An optical device that is made by manipulating the polarization of light and creating a singularity in the polarization, such as Q-plates, produces vortex beams [12], [13]. Recently, an interesting study was done by modulating light with an amplitude RG, which included the geometric shadow in diffraction patterns [8]. In addition, a comprehensive analysis of white light diffraction from radial structures was performed. A white light can generate a colorful rainbow in the intensity pattern after diffraction from an amplitude RG [14].

A comprehensive theoretical analysis gives us a point of view according to reality and an understanding of the nature of propagation and what happens to the beam after diffraction. For example, observing the Talbot effect in the beam pattern of the radial carpet beams makes our analysis simpler when looking at the diffraction pattern from the RG [8], [15].

In this work, the transmission of a plane wave through an MFZG with sinusoidal and binary profiles, a combination of a FZP and an RG, is analyzed theoretically and experimentally. The theoretical analysis uses the Fresnel–Kirchhoff diffraction integral to analytically examine the propagation of plane waves from MFZG with sinusoidal and binary profiles. The experimental analysis involves recording a laser beam's near-field diffraction patterns at specific distances from the grating. The experimental patterns obtained fully validate the analytical results.

II. THEORY

A. *Radial grating*

The RG is a type of periodic diffraction grating with an azimuthal periodicity in the polar coordinate system where its periodicity does not depend on the radial coordinate.

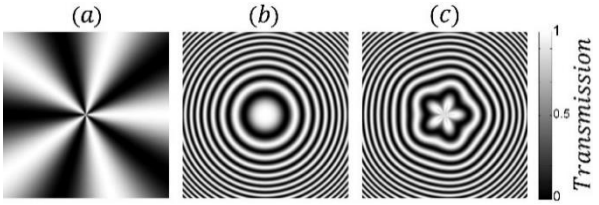

Fig. 1. (a) Amplitude RGs with spoke numbers of $p=5$ having sinusoidal transmission profiles, (b) FZP with a structure constant $s=0.256\,\mathrm{cm}^2$ and (c) an amplitude MFZG with a structure constant $s=0.256\,\mathrm{cm}^2$ and $p=5$. The actual size of all gratings is $4\times4\,\mathrm{cm}^2$.

The structure of this grating is a separable two-dimensional structure in the polar coordinate system, whose components of the transmission function $T(\mathrm{r},\varphi)$ are separable in polar coordinates, that is:

$$T(r,\varphi)=T_R(r)\times T_\varphi(\varphi) \tag{1}$$

where (r,φ) are the polar coordinates in the input plane. As it was said, the transmission function of RG does not depend on the radial coordinate; that is $T_R(r)=1$. The azimuthal part of the transmission function is defined as $T_\varphi(\varphi)$ in Eq. 1. The gratings that affect the incident light by changing the amplitude are called amplitude diffraction gratings. Indeed, these gratings absorb or reflect a part of the radiation wave energy. Amplitude RG is in the form of circle segments that share the circle's center. The equation of the transmission function of the RG with a sinusoidal profile of the amplitude is written as follows:

$$T_{RG}(\varphi)=\frac{1}{2}\left[1+\cos\left(p\varphi\right)\right]=\frac{1}{2}+\frac{1}{4}\left(e^{ip\varphi}+e^{-ip\varphi}\right) \tag{2}$$

where p shows the grating spoke numbers. The visibility of this grating is set to vis=1. Figure 1 (a) shows an example of an amplitude RG with a sinusoidal profile having a spoke number $p = 5$.

B. *Fresnel zone plat (FZP)*

FZP, made of consecutive bright and dark concentric circles with different widths, is a diffractive optical element. The period of this grating depends inversely on the distance from its center. This element has played a significant role in optics in recent years. According to its application and used wavelength, the FZP is made as one-dimensional and two-dimensional symmetrical structures. The phase dependency of the FZP is proportional to the square of the distance from its center. The phase of the patterns does not depend on the azimuthal coordinate and only has a radial dependence in the polar coordinate system. Suppose this quadratic phase dependency in the Cartesian coordinate system depends on only one coordinate. In that case, the created pattern comprises several parallel lines perpendicular to the corresponding axis whose period decreases inversely with the distance from the beginning of the grating. This structure acts like a cylindrical lens in diffraction and has applications such as imaging, focusing X-rays, and making flat antennas.

The equation of the transmission function of a FZP can be written as follows:

$$T_{\mathrm{FZP}}(r) = \frac{1}{2}\left[1 + \cos\left(\frac{\pi}{s} r^2\right)\right] \qquad (3)$$

where λ the wavelength of incident light. We call $s = \lambda f$ the FZP structure constant and f is the farthest focal length from the grating when used as a diffractive lens. Figure 1 (b) shows an FZP with a structure constant $s = 0.256\,\mathrm{cm}^2$ and dimensions of $4 \times 4\,\mathrm{cm}^2$.

C. *Amplitude MFZG with a sinusoidal profile*

A new type of grating is produced by combining the phase dependence of RG and FZP. We define the transmission function of the amplitude MFZG by sinusoidal transmission function as follows:

$$T_S(r,\varphi) = \frac{1}{2}\left\{1 + \cos\left[-\frac{\pi}{s} r^2 + \cos\left(p\varphi\right)\right]\right\} \qquad (4)$$

The term $\cos(p\varphi)$ is related to the azimuthal structure added to the term $-\pi r^2 / s$ that is associated with the phase of the Fresnel pattern. Figure 1 (c) shows an amplitude MFZG with a structure constant $s = 0.256\,\mathrm{cm}^2$ and $p = 5$. In the MFZG transmission function, the FZP phase dependency causes the beam to be focused. In addition, a dependency on the azimuthal angle gives azimuthal periodicity p in the polar coordinates system. Figure 2 shows some examples of this structure with different parameters s and p. In this figure, the number of spokes is 3, 5, and 10. The farthest focal length of the grating for the wavelength of incident beam $\lambda = 532\,\mathrm{nm}$ is 1m and 2m for the first and second rows, respectively, for actual dimensions of the gratings equal $4 \times 4\,\mathrm{mm}^2$. The dimensions of the gratings drawn in the figures differ from the actual size.

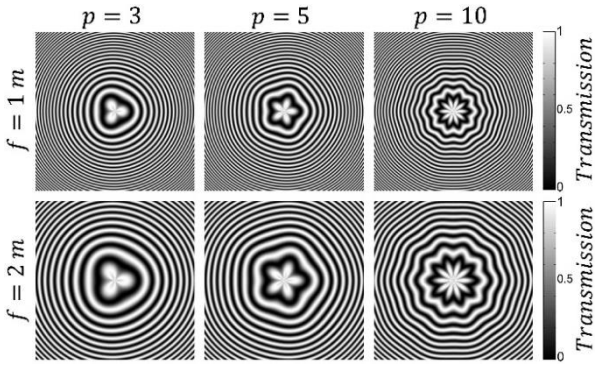

Fig. 2. Transmittance functions for MFZG with different parameters *f* and *p*: incident light assumed to have wavelength $\lambda = 532\,\mathrm{nm}$. The actual size of all gratings is $4 \times 4\,\mathrm{mm}^2$.

Here, we examine this grating with a sinusoidal transmission function. In the following, using the Fresnel-Kirchhoff integral, the near-field diffraction of a plane wave from MFZG, defined as an amplitude grating, is investigated. In addition, the near-field diffraction of a plane wave from these gratings is studied experimentally.

D. *Theoretical analysis of plane wave diffraction from an MFZG with a sinusoidal profile*

Here we investigate the diffraction of plane wave from amplitude MFZG. As mentioned earlier, the basis of the analytical work is the solution of the Fresnel-Kirchhoff integral in the cylindrical coordinate system. By illuminating this amplitude structure with a plane wave, the complex amplitude of the light field after the structure is given by [8]:

$$\begin{aligned} \mathrm{U}(\rho,\theta,z) &= h_0\, \mathrm{e}^{i\alpha\rho^2} \\ &\times \int_0^{\infty}\int_0^{2\pi} dr\, d\varphi r T(r,\varphi) \mathrm{e}^{i\alpha r^2} \mathrm{e}^{-i2\alpha\rho r\cos(\varphi-\theta)} \end{aligned} \tag{5}$$

where ρ is the radial coordinate and θ is the azimuthally angle in the output plane on the screen. Also, $\alpha = \dfrac{\pi}{\lambda z}$, $h_0 = \dfrac{e^{ikz}}{i\lambda z}$ and $k = \dfrac{2\pi}{\lambda}$.

Equation 4 can be expanded using Euler's formula in the following form

$$\begin{aligned} T_S(r,\varphi) &= \frac{1}{2}\left[1+\cos\left(-cr^2+\cos p\varphi\right)\right] \\ &= \frac{1}{4}\left[2+\left(e^{i\left(-cr^2+\cos(p\varphi)\right)}+e^{-i\left(-cr^2+\cos(p\varphi)\right)}\right)\right] \end{aligned} \tag{6}$$

where $c = \pi / s$. By substituting Eq. 6 in Eq. 5, the complex amplitude of the light field after passing from the structure at propagation distance z, we have:

$$\begin{aligned} &\mathrm{U}(\rho,\theta,\mathrm{z}) = \frac{h_0 e^{i\alpha\rho^2}}{4}\times \\ &\times\left\{\int_0^{\infty}\int_0^{2\pi} dr d\varphi r e^{i\alpha r^2} e^{-2i\alpha\rho r\cos(\varphi-\theta)} + \right. \\ &+2\int_0^{\infty}\int_0^{2\pi} dr\, d\varphi r e^{i(\alpha-c)r^2} \mathrm{e}^{i\cos(p\varphi)} e^{-2i\alpha\rho r\cos(\varphi-\theta)} + \\ &\left.+2\int_0^{\infty}\int_0^{2\pi} dr\, d\varphi r e^{i(\alpha+c)r^2} e^{-i\cos(p\varphi)} e^{-2i\alpha\rho r\cos(\varphi-\theta)}\right\} \end{aligned} \tag{7}$$

By using the Jacobi-Anger expansion [16]:

$$e^{i\gamma\cos\theta} = \sum_{m=-\infty}^{+\infty} (i)^m J_m(\gamma) e^{i\theta} \tag{8}$$

where i is the imaginary unit, and J_m is the mth Bessel function of the first kind, and Hankel transform, we have [17]:

$$\begin{cases} H_0\left\{e^{i\alpha r^2}\right\} = 2\pi\int_0^{\infty} e^{i\alpha r^2} J_0(br) r dr \\ H_m\left\{e^{i\alpha r^2}\right\} = 2\pi\int_0^{\infty} e^{i\alpha r^2} J_m(br) r dr \end{cases} \tag{9}$$

or equivalently

$$\begin{cases} H_0\left\{e^{i\alpha r^2}\right\} = \dfrac{i}{2\alpha} e^{\frac{-ib^2}{4\alpha}} \\ H_m\left\{e^{i\alpha r^2}\right\} = \dfrac{b}{4}\left(\dfrac{\pi}{\alpha}\right)^{\frac{3}{2}} e^{-i\left(\frac{b^2}{8\alpha}-\frac{m\pi}{4}\right)} \\ \qquad\qquad \times\left[J_{\frac{m+1}{2}}\left(\dfrac{b^2}{8\alpha}\right)+i\, J_{\frac{m-1}{2}}\left(\dfrac{b^2}{8\alpha}\right)\right] \end{cases} \tag{10}$$

Therefore, using Eqs. 8 and 10 in Eq. 7, the complex amplitude of the light field after the MFZG at a propagation distance of z can be written as follows:

$$\begin{aligned} \mathrm{U}(\rho,\theta,\mathrm{z}) &= \frac{\pi h_0 e^{i\alpha\rho^2}}{2}\left\{\frac{i}{\alpha} e^{\left(\frac{-ib^2}{4\alpha}\right)}\right. \\ &+\sum_{m=-\infty}^{+\infty} (i)^{-\frac{mp}{2}+m} J_m(1) e^{imp\theta} \frac{b}{8\pi}\left(\frac{\pi}{\beta_-}\right)^{\frac{3}{2}} \\ &\times e^{\left(\frac{-ib^2}{8\beta_-}\right)}\left[J_{\frac{mp+1}{2}}\left(\frac{b^2}{8\beta_-}\right)+i\, J_{\frac{mp-1}{2}}\left(\frac{b^2}{8\beta_-}\right)\right] \\ &+\sum_{m=-\infty}^{+\infty} (i)^{-\frac{mp}{2}-m} J_m(1) e^{imp\theta} \frac{b}{8\pi}\left(\frac{\pi}{\beta_+}\right)^{\frac{3}{2}} \\ &\left.\times e^{\left(\frac{-ib^2}{8\beta_+}\right)}\left[J_{\frac{mp+1}{2}}\left(\frac{b^2}{8\beta_+}\right)+i\, J_{\frac{mp-1}{2}}\left(\frac{b^2}{8\beta_+}\right)\right]\right\} \end{aligned} \tag{11}$$

where $b = \dfrac{2\alpha r}{\lambda z}$ and $\beta_{\pm} = \mathrm{c} \pm \alpha$.

Equation 11 describes the complex amplitude of the diffracted light from the MFZG at a propagation distance *z*.

E. *Near-field diffraction of a plane wave from an amplitude MFZG with a binary profile*

The transmission function through an amplitude MFZG with a binary profile in the polar coordinate system can be written as follows:

$$T_B(r,\varphi)=\frac{1}{2}\left\{1+\text{sign}\left[\cos\left(-cr^2+\cos\left(p\varphi\right)\right)\right]\right\} \tag{12}$$

where *c* is the same as defined before, and *r* and φ are the radial and azimuthal angle parameters specified on the grating's plane, respectively. The "sign" is the sign function, and is defined as follows:

$$\text{sign}(x)=\begin{cases}+1 & x>0\\ 0 & x=0\\ -1 & x<0\end{cases} \tag{13}$$

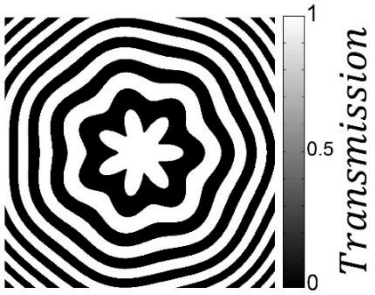

Fig. 3. Presentation of an amplitude MFZG with binary transmission function and spoke number *p*=7 and grating structure constant $s=0.5\,\text{cm}^2$. The actual size of the grating is $4\times4\,\text{cm}^2$

Figure 3 shows the transmission function of a binary type of an MFZG. The transmission function of an amplitude MFZG with a binary profile can be written as a Fourier series. The Fourier coefficients will be as follows [8]:

$$T_B(r,\varphi)=\frac{1}{2}\left\{1+\sum_{t=1}^{\infty}A_t\,e^{i\left[-cr^2+\cos(p\varphi)\right]}+\sum_{t=1}^{+\infty}A_{-t}e^{i\left[-cr^2+\cos(p\varphi)\right]}\right\}=\frac{1}{2}\left\{1+\sum_{t=1}^{\infty}\sin c\left(\frac{\pi t}{2}\right)\times\left[e^{i\left[-cr^2+\cos(p\varphi)\right]}+e^{-i\left[-cr^2+\cos(p\varphi)\right]}\right]\right\} \tag{14}$$

By substituting Eq. 14 in Eq. 5, the complex amplitude of the light field after the grating at a propagation distance of *z*, we have:

$$\begin{aligned}&\mathrm{U}(\rho,\theta,\mathrm{z})=\frac{h_0}{2}\mathrm{e}^{i\alpha\rho^2}\times\\&\left\{\int_0^{\infty}\int_0^{2\pi}\mathrm{e}^{i\alpha r^2}\mathrm{e}^{-2i\alpha\rho r\cos(\varphi-\theta)}r\,dr\,d\varphi+\sum_{t=1}^{+\infty}\text{sinc}\left(\frac{\pi t}{2}\right)\times\right.\\&\int_0^{\infty}\int_0^{2\pi}dr\,d\varphi r\mathrm{e}^{i(\alpha-c)r^2}\mathrm{e}^{i\cos(p\varphi)}\mathrm{e}^{-2i\alpha\rho r\cos(\varphi-\theta)}\\&+\sum_{t=1}^{+\infty}\text{sinc}\left(\frac{\pi t}{2}\right)\times\\&\left.\int_0^{\infty}\int_0^{2\pi}dr\,d\varphi r\mathrm{e}^{i(\alpha+c)r^2}\mathrm{e}^{-i\cos(p\varphi)}\mathrm{e}^{-2i\alpha\rho r\cos(\varphi-\theta)}\right\}\end{aligned} \tag{15}$$

Using the Jacobi-Anger expansion and Hankel transform, the complex amplitude of the light field at a propagation distance of *z* can be written as follows:

$$\begin{aligned}&\mathrm{U}(\rho,\theta,\mathrm{z})=\pi h_0e^{i\alpha\rho^2}\left\{\frac{i}{\alpha}e^{\frac{-ib^2}{4\alpha}}+\right.\\&+\sum_{\mathrm{t}=1}^{+\infty}\sum_{\mathrm{m}=-\infty}^{+\infty}\text{sinc}\left(\frac{\pi\mathrm{t}}{2}\right)(i)^{-\frac{mp}{2}+m}J_m(1)\mathrm{e}^{i\,mp\theta}\\&\frac{b}{8\pi}\left(\frac{\pi}{\alpha_-}\right)^{\frac{3}{2}}e^{\frac{-ib^2}{8\alpha_-}}\left[J_{\frac{mp+1}{2}}\left(\frac{b^2}{8\alpha_-}\right)+i\,J_{\frac{mp-1}{2}}\left(\frac{b^2}{8\alpha_-}\right)\right]\\&+\sum_{\mathrm{t}=1}^{+\infty}\sum_{\mathrm{m}=-\infty}^{+\infty}\text{sinc}\left(\frac{\pi\mathrm{t}}{2}\right)(i)^{-\frac{mp}{2}-m}J_m(1)e^{i\,mp\theta}\\&\left.\frac{b}{8\pi}\left(\frac{\pi}{\alpha_+}\right)^{\frac{3}{2}}e^{\frac{-ib^2}{8\alpha_+}}\left[J_{\frac{mp+1}{2}}\left(\frac{b^2}{8\alpha_+}\right)+i\,J_{\frac{mp-1}{2}}\left(\frac{b^2}{8\alpha_+}\right)\right]\right\}.\end{aligned} \tag{16}$$

where, $b=\dfrac{2\alpha r}{\lambda z}$ and $\beta_{\pm}=\mathrm{c}\pm\alpha$.

The diffraction pattern on the screen is equivalent to the intensity distribution of the light field. Therefore, the intensity must be obtained. The intensity function is produced by multiplying the complex amplitude function of

the light field by its complex conjugate. We draw the intensity profile of the diffracted beam, which is obtained by multiplying the field in its complex conjugate as $I(\rho,\theta) = U(\rho,\theta).U^{*}(\rho,\theta)$, where * denotes the complex conjugate.

III. EXPERIMENTS

A. *Experimental results of plane wave diffraction from amplitude MFZG with a sinusoidal profile*

Figure 4 shows a schematic of the setup for producing diffraction patterns. The light source used is the second harmonic of the Nd:YAG laser beam with diode pumping, which has a Gaussian transverse fundamental mode. A converging lens collimated the divergent laser beam, and its distance was adjusted so that the dimensions of the produced beam were more extensive than the dimensions of the grating until the grating was exposed to the central area of the beam. This will make the beam's wavefront assumed to be the wavefront of a plane wave. Near-field diffraction patterns were recorded using the digital camera sensor without using any lens (Nikon D7200) around the focusing light beam diffracted from the grating Diffraction patterns are recorded at three distances: before, near, and after the gratings' focal length, whose corresponding values are specified in the figures. We produced MFZGs by using the lithography method on transparent film.

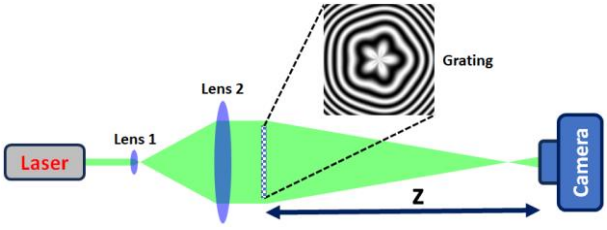

Fig. 4. Schematics of the experimental set-up for producing plane wave diffraction patterns from amplitude gratings. Lens 1 (microlens) and Lens 2 are used together as a beam expander.

In the following, analytical results and experimental results are compared. The results show that the analytical and experimental results are fully compatible.

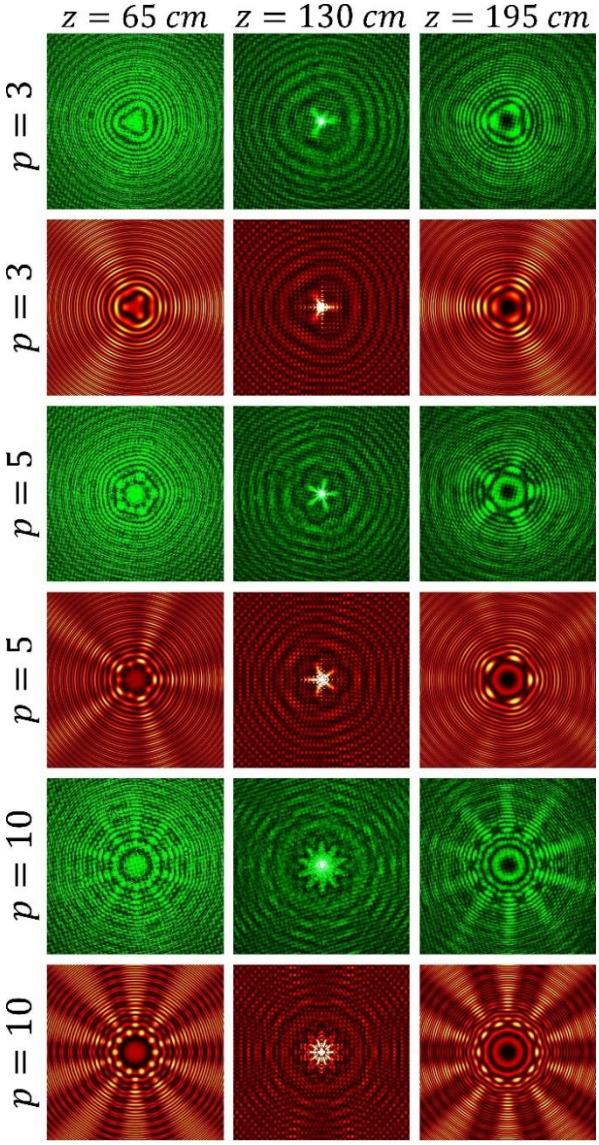

Fig. 5. Experimental recorded results (Green patterns) and analytical results (red patterns) for plane wave diffraction patterns from amplitude MFZG with sinusoidal profiles and spoke numbers p=3, 5, 10 at different distances of z=65, 130, 195cm from the gratings. The focal length of all gratings is considered f =130 cm.

Figure 5 shows the experimental recorded and analytical results for plane wave diffraction patterns of a plane wave from different MFZGs with a sinusoidal profile. Diffraction patterns in the different columns were recorded at propagation distances of z=65cm, 130cm, and 195cm for different gratings with the spoke numbers p=3, 5, and 10. The beam's wavelength used to create all the patterns is $\lambda = 532\,\text{nm}$, and the focal length corresponding to the gratings is $f = 130\,\text{cm}$. Green and red patterns correspond to experimental and analytical results, respectively. The comparison

of the results shows the complete agreement of the analytical and experimental results. In the calculations, the dimensions of the gratings are considered the same as those in the experiments.

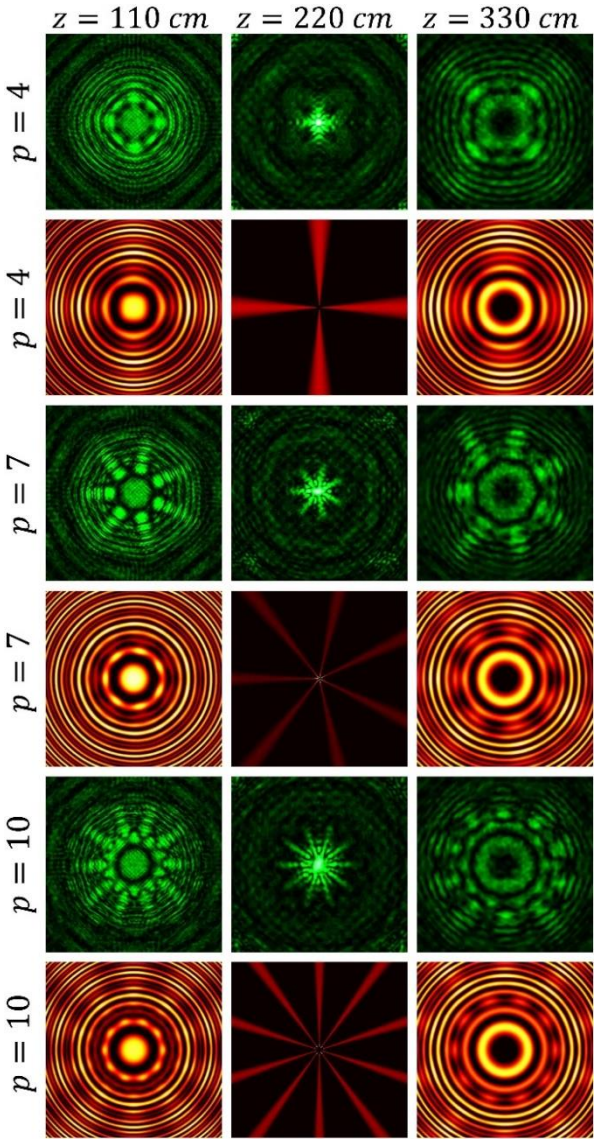

Fig. 6. Experimental recorded results (Green patterns) and analytical results (red patterns) for plane wave diffraction patterns from amplitude MFZG with binary profiles and spoke numbers p=4, 7, 10 at different distances of z=110, 220, 330cm from the gratings. The focal length of all gratings is considered f=220 cm.

Figure 6 shows the experimental recorded and analytical results for plane wave diffraction patterns of a plane wave from different MFZGs with a binary profile. Diffraction patterns in the various columns were recorded at propagation distances of z=110cm, 220cm, and 330cm for different gratings with the spoke numbers p=4, 7, and 10. The beam's wavelength used to record the experimental results was similar to the previous case, but the focal length considered for the gratings is $f = 220\,\text{cm}$. Again, the green and red patterns correspond to experimental and analytical results.

IV. CONCLUSION

The argument of MFZG is a combination of the term $-cr^2$ related to the phase of the Fresnel pattern and the term $\cos(p\varphi)$ related to the radial structure; the term associated with the phase of the Fresnel pattern causes the beam's focus in a certain distance. Due to the presence of the radial term in the MFZG, plane wave diffraction has a pattern similar to the wave diffracted from an RG. By examining the experimental and analytical results, it can be seen that the diffraction pattern becomes focused at a certain distance. Also, by examining the experimental and analytical results, we see that the general shape of the diffraction pattern is more related to the phase of the Fresnel pattern. After and before the focal point, the diffraction pattern behaves similarly to the diffraction pattern of a Fresnel grating. Comparing the recorded experimental patterns and those obtained from the theoretical investigations drawn with the MATLAB program shows that the theoretical predictions agree with the experimental results.

Similar to diffraction from other radial shapes, various applications can be considered due to the creation of a high-intensity alternating lobe on the target plane, including optical tweezers, optical manipulation, and beam shaping. Perhaps, in the future, the investigation of diffraction patterns from structures based on radial structures will create the basis for the construction of systems that act as transmitters-receiver based on wavefront topology. This lookout opens a new goal to enter the new world, where the topology of the structures plays a vital role in transmitting information even without considering the wave nature.

REFERENCES

[1] S.A. Akhmanov and S.Y. Nikitin, *Physical Optics*, Oxford University Press, pp. 3-20, 1997.

[2] J.W. Goodman, *Introduction to Fourier optics*, 3rd ed., Roberts and Company publishers, pp. 173-216, 2005.

[3] J. Alonso and E. Bernabeu, "Spatial evolution of Gaussian beams diffracted by radial gratings," Opt. Commun., Vol. 98, pp. 323-330, 1993.

[4] S. Rasouli and D. Hebri, "Contrast enhanced quarter Talbot images," J. Opt. Soc. Am. A, Vol. 35, pp. 2145-2156, Nov. 2017.

[5] S. Rasouli, F. Sakha, and M. Yeganeh, "Infinite-mode double-grating interferometer for investigating thermal-lens-acting fluid dynamics," Meas. Sci. Technol., Vol. 29, pp. 085201(1-11), 2018.

[6] S. Rasouli, M. Dashti, and A.N. Ramaprakash, "An adjustable, high sensitivity, wide dynamic range two channel wave-front sensor based on moiré deflectometry," Opt. Express, Vol. 18, pp. 23906-23915, 2010.

[7] M.C. Hettrick and S. Bowyer, "Variable line-space gratings: new designs for use in grazing incidence spectrometers," Appl. Opt., Vol. 22, pp. 3921-3924, 1983.

[8] S. Rasouli, A.M. Khazaei, and D. Hebri, "Talbot carpet at the transverse plane produced in the diffraction of plane wave from amplitude radial gratings," J. Opt. Soc. Am. A, Vol. 35(55), pp. 55-64, 2018.

[9] V. Moreno, J.F. Román, and J.R. Salgueiro, "High efficiency diffractive lenses: deduction of kinoform profile," Am. J. Phys., Vol. 65, pp. 556-562, 1997.

[10] M. Mihailescu, A. Preda, D. Cojoc, E. Scarlat, and L. Preda, "Diffraction patterns from a phyllotaxis-type arrangement," Opt. Lasers Eng., Vol. 46(11), pp. 802-809, 2008.

[11] A.M. Yao and M.J. Padgett, "Orbital angular momentum: origins, behavior and applications," Adv. Opt. Photon., Vol. 3, pp. 161-204, 2011.

[12] D.L. Andrews and M. Babiker, The angular momentum of light, Cambridge University Press, pp. 51-70, 2012.

[13] L. Marrucci, "The q-plate and its future," J. Nanophoton., vol. 7, pp. 078598-078598, 2013.

[14] S. Rasouli, S. Hamzeloui, and D. Hebri, "Colorful radial Talbot carpet at the transverse plane," Opt. Express, Vol. 27, pp. 17435-17448, 2019.

[15] S. Rasouli and A.M. Khazaei, "An azimuthally-modified linear phase grating: generation of varied radial carpet beams over different diffraction orders with controlled intensity sharing among the generated beams," Sci. Rep., Vol. 9, pp. 12472, 2019.

[16] G.B. Arfken and H.J. Weber, *Mathematical Methods for Physicists*, 6th ed., Academic Press, pp. 687, 2005.

[17] A. Jeffrey and D. Zwillinger, "Table of integrals, series, and products", 7th ed., Elsevier Inc., pp. 739-739, 2007.

Ali Mohammad Khazaei received his BSc in physics from Islamic Azad University, Khorramabad Branch, Khorramabad, Iran, in 2006 and his MSc in physics from Imam Hossein University, Tehran, Iran, in 2011. He obtained his PhD in Physics from the Institute for Advanced Studies in Basic Sciences (IASBS) Physics Department in Zanjan, Iran, in 2019. He completed a postdoctoral research course in the Institute for Advanced Studies in Basic Sciences (IASBS) Physics Department in Zanjan, Iran, in 2022. From 2022, he was an assistant professor at Lorestan University, Khorramabad, Iran. His research interests include diffractive optics, structured light, and singular optics.

Fatemeh Afsharipour received her BSc in physics from Shahid Bahonar University, Kerman, Iran, in 2021 and her MSc degree in optics and laser from Shahid Bahonar University, Kerman, Iran, in 2024. She works as a researcher at the structured light Laboratory in the Department of Physics, Shahid Bahonar University, Kerman, Iran. Her primary research interest lies in diffraction and structured light.

Hamid Reza Mashayekhi was born in Tonekabon, Mazandaran, Iran, in 1965. He pursued his passion for physics by obtaining a BSc at the University of Mashhad in 1992. He continued his academic journey supported by a scholarship, culminating in an MSc and PhD from the University of Essex, UK. Specializing in Optical Communication Systems and Semiconductor Physics, Dr. Mashayekhi currently serves as an assistant professor at Shahid Bahonar University of Kerman, dedicating himself to academic excellence. With a solid commitment to research and teaching, he inspires future optics and semiconductor physics by engaging in projects to advance knowledge in Laser technology.

Mohammad Yeganeh was born in Tabriz-Iran in 1981. He received his BSc and MSc degrees from the University of Tabriz, Iran, in 2003 and 2006, respectively. He was granted his PhD in physics, specializing in optics from the Institute for Advanced Studies in Basic Sciences (IASBS) Physics Department in Zanjan, Iran, in 2016. He completed a postdoctoral research course in same institution the Institute for.

He is now an assistant professor at the Department of Physics Education, Farhangian University in Tabriz, Iran. His most critical professional interests are the Moiré technique, singular optics, optics of liquid crystals, atmospheric turbulence, optical metrology, and optical design.

Dr Yeganeh has been a member of the “Physics Society of Iran” and the “Optics and Photonics Society of Iran” since 1999 and 2009, respectively. He got the “9th Alimohammadi Prize” for his outstanding PhD thesis in physics from IPM in Iran in June 2019. He is a “Trusted Reviewer status” in the IOP.

THIS PAGE IS INTENTIONALLY LEFT BLANK.